Atmospheric Science Letters (2000) Volume 1
doi:10.1006/asle.2000.0004

Simulation of the Asian Summer Monsoon in Five European General Circulation Models

G. M. Martin[1], K. Arpe[2], F. Chauvin[3], L. Ferranti[4], K. Maynard[5], J. Polcher[5], D. B. Stephenson[3] and P. Tschuck[2]

[1]*Hadley Centre for Climate Prediction and Research, The Met. Office, Bracknell, U.K.*
[2]*Max Planck Institute for Meteorology, Hamburg, Germany*
[3]*Meteo-France Centre National de Recherches Meteorologiques, Toulouse Cedex, France*
[4]*European Centre for Medium-range Weather Forecasting, Shinfield Park, Reading, U.K.*
[5]*Laboratoire de Meteorologie Dynamique, Paris, France*

Abstract: A comparison is made of the mean monsoon climatology in five different general circulation models (GCMs) which have been used by the participants of a project, funded by the European Union, entitled Studies of the Influence, Hydrology and Variability of the Asian summer monsoon (SHIVA). The models differ considerably, in horizontal and vertical resolution, numerical schemes and physical parametrizations, so that it is impossible to isolate the cause of differences in their monsoon simulations. Instead, the purpose of this comparison is to document and compare the representation of the mean monsoon in models which are being used to investigate the characteristics of the monsoon, its variability and its response to different boundary forcings. All of the models produce a reasonable representation of the monsoon circulation, although there are regional variations in the magnitude and pattern of the flow at both 850 hPa and 200 hPa. Considerable differences between the models are seen in the amount and distribution of precipitation. The models all reproduce the basic monsoon seasonal variation, although the timing of the onset and retreat, and the maxima in the winds and precipitation during the established phase, differ between them. There are corresponding differences in the evolution of the atmospheric structure between the pre-monsoon season and its established phase. It is hoped that this study will set in context the investigations of the monsoon system and its impacts carried out using these models, both during SHIVA and in the future.

Keywords: Asian summer monsoon; general circulation models; SHIVA.

1. INTRODUCTION

The simulation of the Asian Summer Monsoon (ASM) and its variability remains a significant challenge for general circulation models (GCMs). The ASM is a major component of the atmospheric circulation, and the economies and livelihood of the populations of India and southeast Asia depend heavily on the rainfall associated with it. In order for these countries to benefit from seasonal predictions of

1530-261X

monsoon rainfall, it is essential that GCMs are able to produce a reasonable simulation of both the mean monsoon circulation and rainfall distribution, and its intraseasonal and interannual variability. In addition, such GCMs are used both to simulate the present climate and to predict future global and regional climate change, so it is essential that the main features of the general circulation are simulated with reasonable accuracy.

The SHIVA project was initiated in 1996 and ran for 3 years, involving scientists from all of the major modelling groups within Europe. The project focused on documenting the observed behaviour of the monsoon, on improving its simulation in climate models, and on assessing the predictability of the system and the factors that might determine that predictability. Details of the monsoon studies carried out during SHIVA can be found in the SHIVA Final Report (Slingo *et al.*, 1999; a review of this book is in the June issue of "Euroabstracts", which can be found at http://www.cordis.lu/euroabstracts). Additional information about the monsoon, as well as links to other sites, can be found at the SHIVA web site at http://www.met.rdg.ac.uk/shiva/shiva.html and at http://www.met.reading.ac.uk/cag/Monsoon/index.html. A comprehensive description of the mean monsoon and its variability was compiled in the SHIVA Atlas, which can also be obtained from the SHIVA web site.

A number of different GCMs were used in the project. In this paper, we compare the monsoon climatologies between the participating models, in order to provide both an indication of the state of the representation of the Asian monsoon in current climate models, and a reference point for individual studies using each of the different models. The five GCMs used are:

(a) climate version HadAM3 (Pope *et al.*, 2000) of The Met. Office (U.K.) Unified Model;
(b) the ARPEGE-Climat model Cycle 18c (an updated version of that used by Stephenson *et al.* (1998), including a statistical cloud scheme (Ricard and Royer, 1993) and a semi-Lagrangian advection scheme) from the Centre National de Recherches Meteorologiques (CNRM) at Meteo-France;
(c) the ECHAM 4.5 model, an updated version of ECHAM4 (Roeckner *et al.*, 1996) from the Max Planck Institute (MPI) for Meteorology, Hamburg, Germany. Changes from ECHAM4 include an implicit treatment of the land surface temperatures, a reduction in the low wind speed correction for unstable conditions over sea, changes to convective precipitation, organized entrainment and CAPE closure time scale, an increase in cloud droplet number concentration, an increase in gravity wave drag and an increase in the minimum relative humidity for condensation at upper levels;
(d) the European Center for Medium-range Weather Forecasting (ECMWF) model version CY18R6; compared with version CY13R4 used by Ferranti *et al.*, (1999), CY18R6 includes a 2-time-level semi-Lagrangian advection scheme as well as increased vertical resolution in the boundary layer and stratosphere; and
(e) the LMD6 model (Polcher and Laval, 1994) from the Laboratoire de Meteorologie Dynamique (LMD), Paris, France.

For four of the models, 17-year runs were carried out as part of the second Atmospheric Model Intercomparison Project (AMIP-II; Gates, 1992). These were forced with observed sea surface temperatures (SSTs) and sea ice data for 1979 to 1995, prepared, using available in-situ, climatological, and satellite data, by the Program for Climate Model Diagnosis and Intercomparison (PCMDI). The run with the ECMWF model was continued on to 1998 using SSTs from the ECMWF operational analyses (based on Reynold values). In the run with the ARPEGE model, the SSTs used in three particular years (1981, 1984 and 1991) were erroneously those of the preceding years (1980, 1983 and 1990). Although this will have little effect on the climatology of the model, these three years have been omitted from the calculation of interannual variability in monsoon onset date in section 6 (there may still be some effect on the interannual variability of using erroneous initial conditions in 1982, 1985 and 1992, although it is likely that this will have less effect than that of using relatively

small samples in all of the models for the analysis of this variability). A ten-year run of the LMD model from 1979 to 1988 was supplied. This run was forced by observed SSTs and sea ice data from the Global sea-Ice and Sea Surface Temperature (GISST2.2) dataset (Rayner *et al.*, 1996), in which in situ data, climatological and bias-adjusted satellite data are combined.

A monsoon region can be defined (Asnani, 1993) as an area in which the Inter-Tropical Convergence Zone (ITCZ) has a large annual oscillation in position. Over Asia, the ITCZ penetrates northwards during the northern summer, extending as far as 45°N over North China in July. Over India and southeast Asia, it extends as far north as Kashmir and the central Tibetan Plateau, and it is bounded to the west by Pakistan and the Rajasthan desert. The north-south movement of the ITCZ is associated with seasonal changes in surface temperature, wind direction, relative humidity and rainfall. Thus, we examine the simulation of these quantities during the monsoon season in the five GCMs. Monthly and seasonal (May to September) averages over the length of each model run are used. In addition, the dates of monsoon onset across the Asian monsoon region have been analysed using daily averages of precipitation and horizontal winds. The model results are compared with similar fields from the ECMWF Re-Analysis (ERA; Gibson *et al.*, 1997) and the NOAA Climate Prediction Center (CPC) Merged Analysis of Precipitation (CMAP/O) produced by Xie and Arkin (1997).

2. DESCRIPTION OF MODELS USED

The models differ in resolution, numerics and physical parametrizations. A summary of each of the models is given in Table 1. With so many differences between the models, it is impossible to isolate the cause of differences in their monsoon climatologies, and this is not the purpose of this comparison. Instead, we focus on documenting the performance of each model in simulating the Asian monsoon. However, the impact of some of the more recent changes made to these models is discussed in section 3.

3. SEASONAL AVERAGES

Figures 1, 2 and 3 show the seasonal (May–September, MJJAS) mean horizontal winds at 850 hPa and 200 hPa, and precipitation, averaged over the length of each of the model runs, compared with climatologies from ERA and CMAP/O. All of the fields have been interpolated onto the 3.75° (longitude) by 2.5° (latitude) grid of the UKMO model, HadAM3, to facilitate the comparison.

All of the models represent the pattern of the monsoon circulation well, in terms of the locations of the westerly Somali jet at 850 hPa and the upper level easterly flow, although the turning of the 850 hPa westerly flow northeastwards around the southern Indian peninsula into the Bay of Bengal is only captured by ECMWF and ECHAM4.5. However, there are considerable variations between the models in the strength of the flow at both levels. Both HadAM3 and LMD6 overestimate the strength of the monsoon circulation, with 850 hPa winds in the jet core over the Arabian Sea exceeding those in ERA by more than 4 m/s. This is a known systematic error in both of these models. Martin and Soman (2000) showed that the monsoon circulation was strengthened in HadAM3 with respect to the previous version of the model, HadAM2b (where it was already too strong) by the inclusion of both the Edwards-Slingo radiation scheme and convective momentum transport (CMT; Gregory *et al.*, 1997). In LMD6, it was found that decreasing the height of the Tibetan Plateau by 50% improved the simulation of the monsoon circulation, and it was suggested that this is related to too strong convergence over the southwestern slopes of the Tibetan Plateau with the standard orography (see section 3, Annex C of Slingo *et al.*, 1999). LMD6 also overestimates the 850 hPa windspeed by more than 8 m/s over southeast Asia, and the 200 hPa windspeed by more than 6 m/s over

Table 1. Summary of SHIVA models

	UKMO	LMD	MPI	CNRM	ECMWF
Model version	HadAM3	LMD6	ECHAM4.5	ARPEGE Cycle 18c	CY18R6
Experiment years	1979–1995	1979–1988	1979–1995	1979–1995	1979–1998
Horizontal resolution	Gridpoint 3.75 × 2.5 deg	Gridpoint 3.75 × sin(lat) deg	Spectral T42. Physics on 2.8 × 2.8 deg Gaussian grid	Spectral T63. Physics on 2.8 × 2.8 deg Gaussian grid	Spectral T63. Physics on 2 × 2 deg grid
Vertical resolution	19 levels	15 levels	19 levels	45 levels	60 levels
Numerical scheme	Conservative split-explicit timestep = 30 mins	Leap-frog scheme, timestep = 6 mins, physics timestep = 24 mins	Semi-implicit, timestep = 24 mins	Semi-implicit, timestep = 30 mins	Semi-implicit, timestep = 60 mins
Advection	4th order Eulerian		Semi-Lagrangian for humidity variables	Semi-Lagrangian	Semi-Lagrangian
Radiation	General 2-stream scheme (Edwards and Slingo, 1996). Separate ice and water; aerosols	SW: Fouquart and Bonnel, 1980; LW: Morcrette *et al.*, 1986.	SW: Fouquart and Bonnel, 1980; LW: Morcrette *et al.*, 1986	Morcrette scheme (Morcrette, 1990)	Morcrette scheme (Morcrette, 1990)
Clouds	Statistical; diagnose cloud water, ice and fraction using RH (Smith, 1990)	Prognostic liquid, water and ice. Statistical condensation	Sunqvist-type, prognostic LWC, diagnosed cloud fraction	Statistical cloud scheme (Ricard and Royer, 1993)	Prognostic cloud water, ice and fraction (Tiedtke, 1993)
Convection	Mass-flux, stability-dependent closure (Gregory and Rowntree, 1990)	Mass-flux; modified Kuo-type (moisture convergence and stability closure)	Mass-flux, CAPE-based closure	Mass-flux; Kuo-type (Bougeault, 1985)	Mass-flux (Tiedtke, 1993)
Boundary layer	Stability-dependent with diagnosed mixing length (Smith, 1990)	Stability-dependent with diagnosed mixing length	1.5 order closure. Eddy diffusivity a function of prognostic TKE	Stability-dependent with diagnosed mixing length	K-profile formulation for dry mixed layer, separate entrainment (Beljaars and Viterbo, 1998)
Surface	4 layers. Freeze and melt soil water; interactive canopy resistance (MOSES, Cox *et al.*, 1999)	7 soil layers, 7 vegetation types. 2 moisture reservoirs (Ducoudre *et al.*, 1993)	5-layer model. 2 moisture reservoirs (Roeckner *et al.*, 1992)	4-layer soil model. 3 moisture reservoirs (Noilhan and Planton, 1989)	4-layer soil model (Viterbo and Beljaars, 1995)

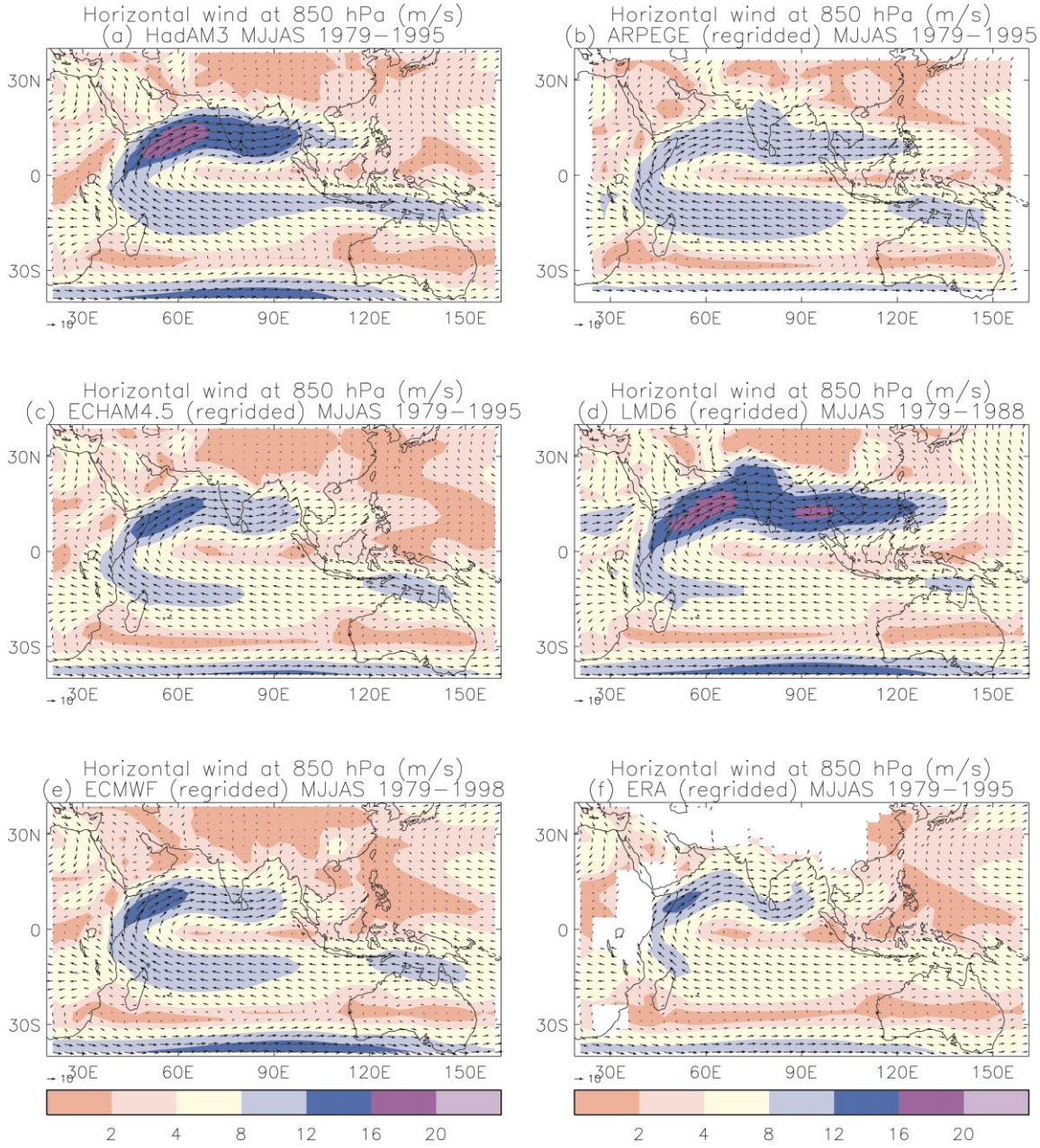

Figure 1. Seasonal (MJJAS) mean climatology of 850 hPa horizontal wind (m/s) for the five SHIVA models and ERA.

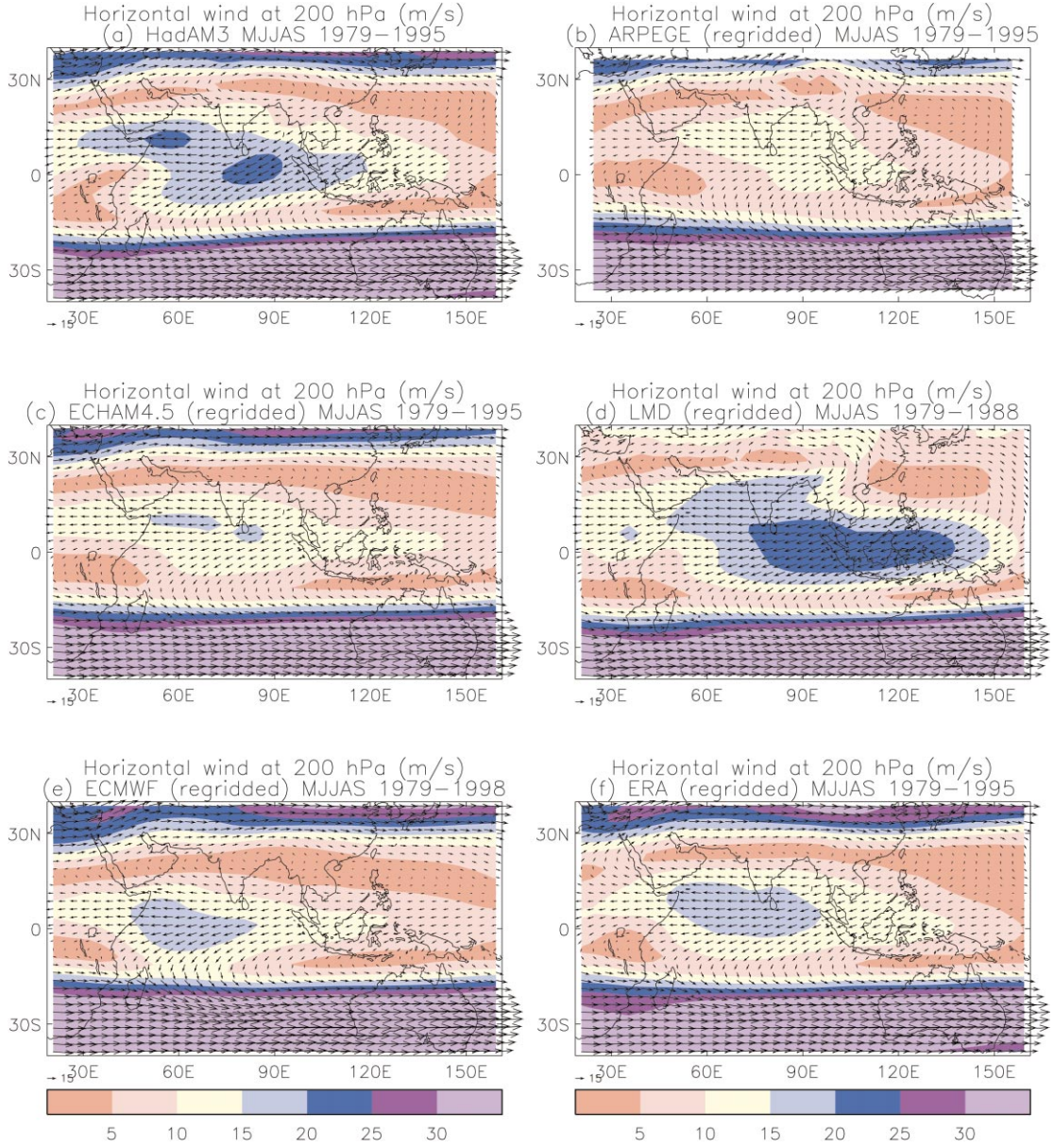

Figure 2. Seasonal (MJJAS) mean climatology of 200 hPa horizontal wind (m/s) for the five SHIVA models and ERA.

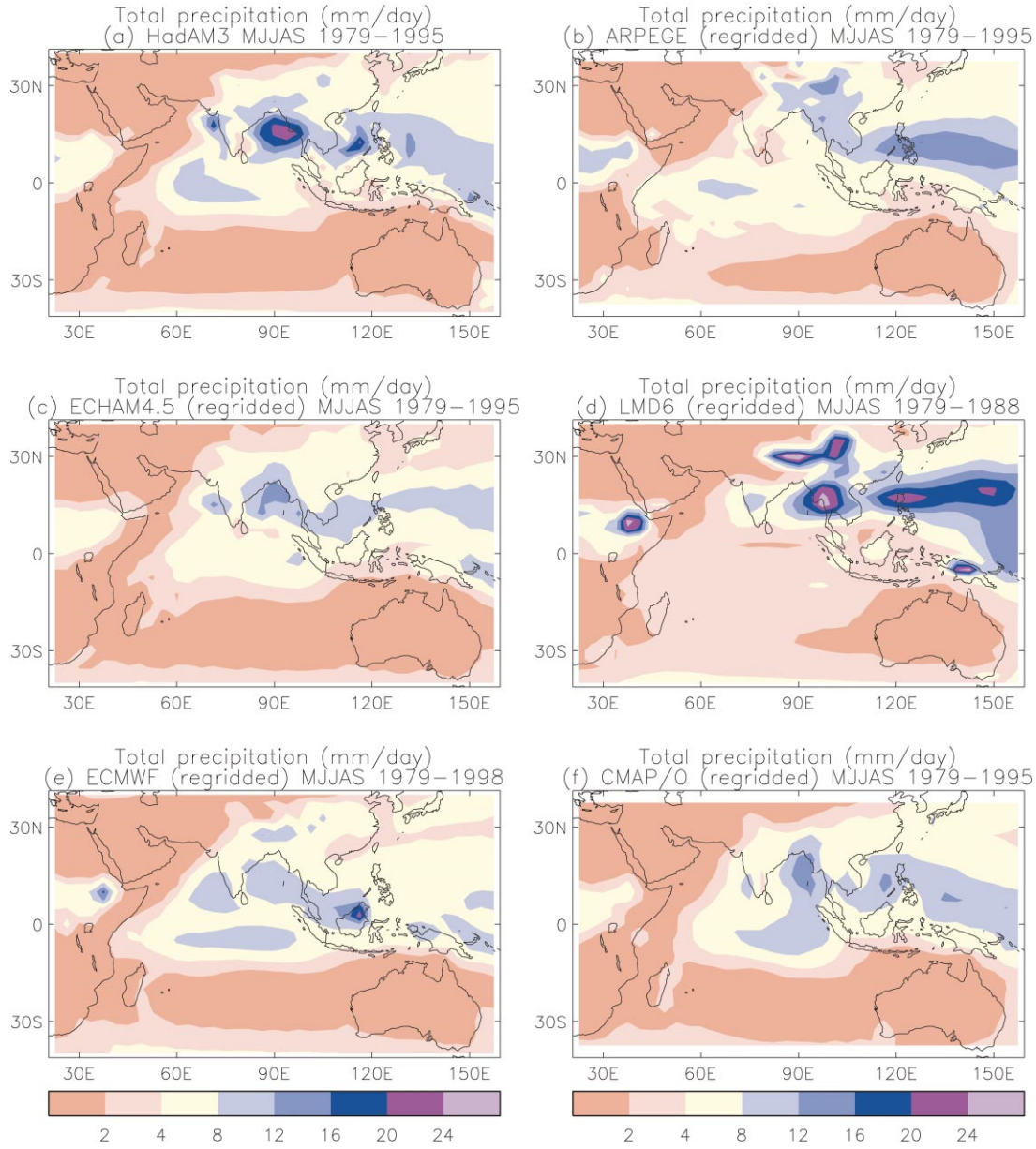

Figure 3. Seasonal (MJJAS) mean precipitation climatology (mm/day) for the five SHIVA models and ERA.

Indonesia. Also in LMD6, the Tibetan anticyclone is further northwest than in the other models or ERA; this is associated with increased easterly flow over India at 200 hPa. Changing the height of the Tibetan Plateau does not appear to alleviate these problems.

The 850 hPa flow is also slightly too strong (by up to around 2 m/s) in ARPEGE (except over the Arabian Sea), ECHAM4.5 and ECMWF, but in the former two models the 200 hPa flow is too weak by up to 4 m/s. With a previous version (version 2) of ARPEGE-Climat, described by Stephenson *et al.*, (1998), the monsoon circulation (at T63) was slightly too strong at both upper and lower levels, although the extension of the westerly flow across southeast Asia to the Philippines at 850 hPa was not present. The weakening of the monsoon circulation in the current model version is thought to be associated with inclusion of the semi-Lagrangian advection scheme (M. Deque, personal communication). The extension of the westerly flow across southeast Asia may be associated with increases in precipitation in this region (see below).

The errors in the monsoon circulation in ECHAM4.5 are much smaller than in the previous version, ECHAM4, where the monsoon circulation was too weak at both lower and upper levels. One of the main contributors to this is the inclusion of an implicit treatment of the land surface temperatures, in which temperatures in the atmosphere and soil are calculated simultaneously and in which energy is conserved (Slingo *et al.*, 1999, section 1.2 of Annex D). Changes to the convection and condensation schemes have also had an impact through redistribution of the convective precipitation (see below).

It should be noted that Annamalai *et al.*, (1999) showed differences in the strength of the Somali jet between ERA and the NCEP/NCAR reanalyses of up to 5 m/s, as well as differences in the pattern of flow over the Indian peninsula and over the Indian Ocean. In addition, the equatorial easterly flow at 200 hPa was systematically stronger in NCEP/NCAR than in ERA. Since these regions are data-sparse, it is not clear which of these is closer to reality. However, HadAM3 and LMD still overestimate the strength of the low-level flow and ARPEGE, ECHAM4.5 and ECMWF underestimate the strength of the upper level flow compared with both reanalyses.

The models exhibit differences in precipitation which are in broad agreement with the differences in circulation. Incorrect representation of the strength of the monsoon circulation is associated with errors in moisture transport into the region, leading to problems with simulating precipitation. For example, the amount of precipitation is overestimated in HadAM3 and LMD6. The latter shows particularly large rainfall amounts over East Asia and the western Pacific, which are associated with the increased 850 hPa flow over this region and the increased upper level flow to the south in Figure 2(d). In HadAM3, the rainfall over western India is concentrated over Gujarat, but this model does represent the rain shadow region seen in CMAP/O over southeast India. Martin and Soman (2000) showed that the concentration of precipitation over Gujarat in HadAM3 is associated with the inclusion of CMT, through increased convergence in this region resulting from changes in the balance of momentum mixing between the convection and boundary layer schemes.

Rainfall in the Indian region is also rather overestimated by ECHAM4.5, although by a smaller amount than in HadAM3. The rain shadow region of southeast India is also represented in this model. Over the western Pacific, the rain band in ECHAM4.5 is further north than in the observations, and the amount of rainfall is slightly underestimated. In ECHAM4, precipitation in the Indian region was underestimated considerably, whilst being excessive over the Indian Ocean and South China Sea. A reduction in the low wind speed correction for unstable conditions over sea made in ECHAM4.5 reduced precipitation over the equatorial Indian Ocean and increased it over India, through a reduction in evaporation over the sea (Slingo *et al.*, 1999, section 1.2 of Annex D). Changes to the depth threshold for precipitation in land-based convection and reductions in the organized entrainment into convection tend to strengthen convection over the land areas, with a compensating reduction over the sea. Finally, the alterations to the condensation scheme lead to enhanced convection over land through changes to the radiative heating of the surface.

Overall, rainfall amounts in the Indian region are overestimated in the ECMWF model. This contrasts with previous versions of the model (without the 2-time-level semi-Lagrangian advection and at lower vertical resolution), in which precipitation in the Indian region was underestimated. However, CY18R6 underestimates precipitation significantly over the Bay of Bengal and the western Pacific, in a similar manner to CY13R4. This may be associated with the lack of convergence in this region in the 850 hPa winds (Figure 2(e)). In contrast, ARPEGE underestimates rainfall in the Indian region and over the eastern part of the equatorial Indian Ocean significantly whilst slightly overestimating the rainfall over the western Pacific. This is in agreement with the rather weak Somali jet over the Arabian Sea and the extension of westerly winds into the western Pacific in this version of the model. As shown in Slingo *et al.*, (1999, section 2.1 of Annex A), the inclusion of the statistical cloud scheme affects convective activity indirectly through its interaction with turbulence and radiative transfer. It was found to result in reduced precipitation over much of the Indian region and increased precipitation in the equatorial Pacific. When the semi-Lagrangian advection scheme was also included, these changes were enhanced as the circulation weakened, although the rainfall over the western part of the equatorial Indian Ocean was increased.

LMD6, ARPEGE and ECMWF also appear to exhibit erroneous precipitation over the southern slopes of the Tibetan Plateau. This is a common problem in GCMs (Gadgil and Sajani, 1998). Lack of observational data in this region makes this result difficult to verify, and Stephenson *et al.*, (1998) noted that the CMAP/O dataset may underestimate the amount of precipitation in this region as it was not gauge-corrected over orography. However, Stephenson *et al.*, (1998) also showed that using low resolution (T21) orography in the higher resolution run of ARPEGE-Climat version 2 reduced the excessive rainfall over the southern slopes of the Tibetan Plateau considerably. Reducing the height of the Tibetan Plateau by 50% in LMD6 also reduced the excessive rainfall in this region, shifting it to the south so that it was more evenly spread over India but still rather excessive over southeast Asia (Slingo *et al.*, 1999, section 3.2 of Annex C). Both of these studies suggest that the treatment of orography in this region and its effects on the atmosphere are crucial to the monsoon simulation.

All of the models, and particularly LMD6, underestimate rainfall amounts over the equatorial Indian Ocean, and in those models which produce more rainfall in this region, the maximum in precipitation is further west than in CMAP/O.

In order to make a quantitative comparison between the models' representation of the Asian monsoon climatology, pattern correlations and root-mean-square (RMS) errors in the zonal winds (U) at 850 hPa and 200 hPa and the precipitation (PPN) are presented in Table 2. Because of the regional nature of the monsoon precipitation, the correlations and RMS errors have been calculated for three subregions as well as for the region as a whole. The latitude/longitude limits of all of the regions used are indicated in Table 2.

The pattern correlations are high for the zonal winds at both upper and lower levels, which is to be expected given that the monsoon circulation is a major component of the general atmospheric circulation. Poorer correlation of the 200 hPa zonal wind is seen in those models in which the location of the easterly jet core differs substantially from that in the reanalyses (e.g. LMD6). The RMS errors illustrate the incorrect strength of the monsoon circulation, even in those models for which the pattern correlations are high (e.g. HadAM3), whilst problems with both the strength and position of the upper and lower level jets are seen in LMD6 and ARPEGE.

The pattern correlations for precipitation are lower than those for the zonal winds because of its regionality. The problems in the precipitation distribution in some of the models, discussed above, are reflected in the correlations, with LMD6 and the ECMWF model showing lower correlations than the other three models. The RMS errors are similar for all of the models except LMD6, which was shown to overestimate the amount of precipitation over much of the region east of 90°E in Figure 3. The correlations and RMS errors for the three subregions give more detail as to where the main problems are, with LMD6 showing particular problems in the Indian region, HadAM3, ARPEGE, LMD6 and ECMWF in the Bay of Bengal region and ARPEGE, LMD6 and ECMWF in the East Asian region. The use of relatively small subregions in this analysis is a tough test of the model simulations, but is useful in highlighting regional problems.

Table 2. Pattern correlations and RMS errors for the five SHIVA models with respect to ERA (for U(850) and U(200)) and CMAP/O (for precipitation)

	HadAM3	ARPEGE	ECHAM4.5	LMD6	ECMWF
U(850) m/s 40–120°E 15°S–20°N					
Corr.	0.964	0.967	0.980	0.924	0.978
RMSE	3.562	2.571	1.626	4.498	1.799
U(200) m/s 40-120E 15S-20N					
Corr.	0.902	0.842	0.986	0.751	0.828
RMSE	3.361	5.511	2.178	5.937	3.754
PPN (mm/day) 60-150E 5-30N					
Corr.	0.674	0.624	0.609	0.272	0.493
RMSE	2.850	2.817	2.487	5.773	2.826
PPN India 75-85E 5-30N					
Corr.	0.527	0.610	0.562	0.240	0.831
RMSE	3.306	2.477	2.289	3.245	2.068
PPN B. Bengal 85-100E 10-30N					
Corr.	0.702	−0.490	0.654	−0.140	0.208
RMSE	5.139	4.941	2.440	8.615	3.390
PPN E. Asia 100-115E 5-30N					
Corr.	0.441	0.287	0.490	−0.282	0.334
RMSE	2.592	2.625	2.000	6.392	2.704

4. SEASONAL EVOLUTION OF THE MONSOON

Timeseries of monthly mean winds and precipitation, averaged over different parts of the monsoon region, are shown in Figure 4. These allow the representation of the monsoon seasonal evolution in the different models to be compared. In ERA, the increase in westerly winds at 850 hPa and easterly winds at 200 hPa associated with the onset of the monsoon over the different regions is evident in June, coinciding with a sharp increase in the precipitation in CMAP/O. The main monsoon activity occurs between July and August, with the monsoon retreating in September.

The models all reproduce the basic monsoon seasonal variation, although the timing of the onset and retreat, and the maxima in the winds and precipitation during the established phase, differ between the models. The overactive monsoon in LMD6 and HadAM3 persists through the season, and is associated with early monsoon onset (as far as can be assessed using monthly averages) and, in the case of LMD6, a late retreat (except over India). ECHAM4.5 shows reasonable agreement with CMAP/O and ERA, except in overestimating the precipitation over India during the established phase of the monsoon. This is also seen in ECMWF, although the circulation is generally weaker than in ERA and the monsoon retreat shows a tendency to be early. With ARPEGE, the monsoon onset is late and the retreat is

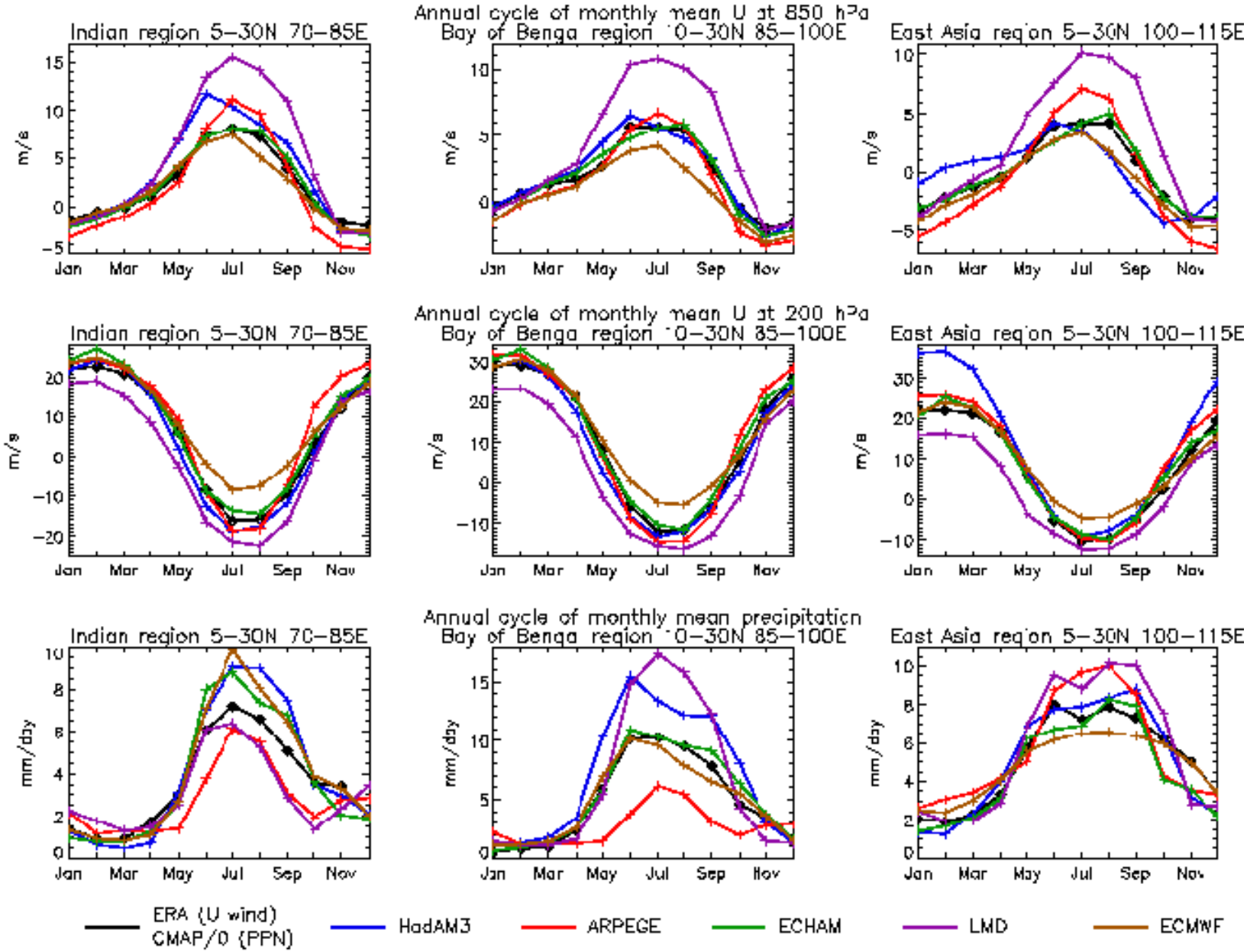

Figure 4. Timeseries of monthly mean winds and precipitation for the five SHIVA models and ERA.

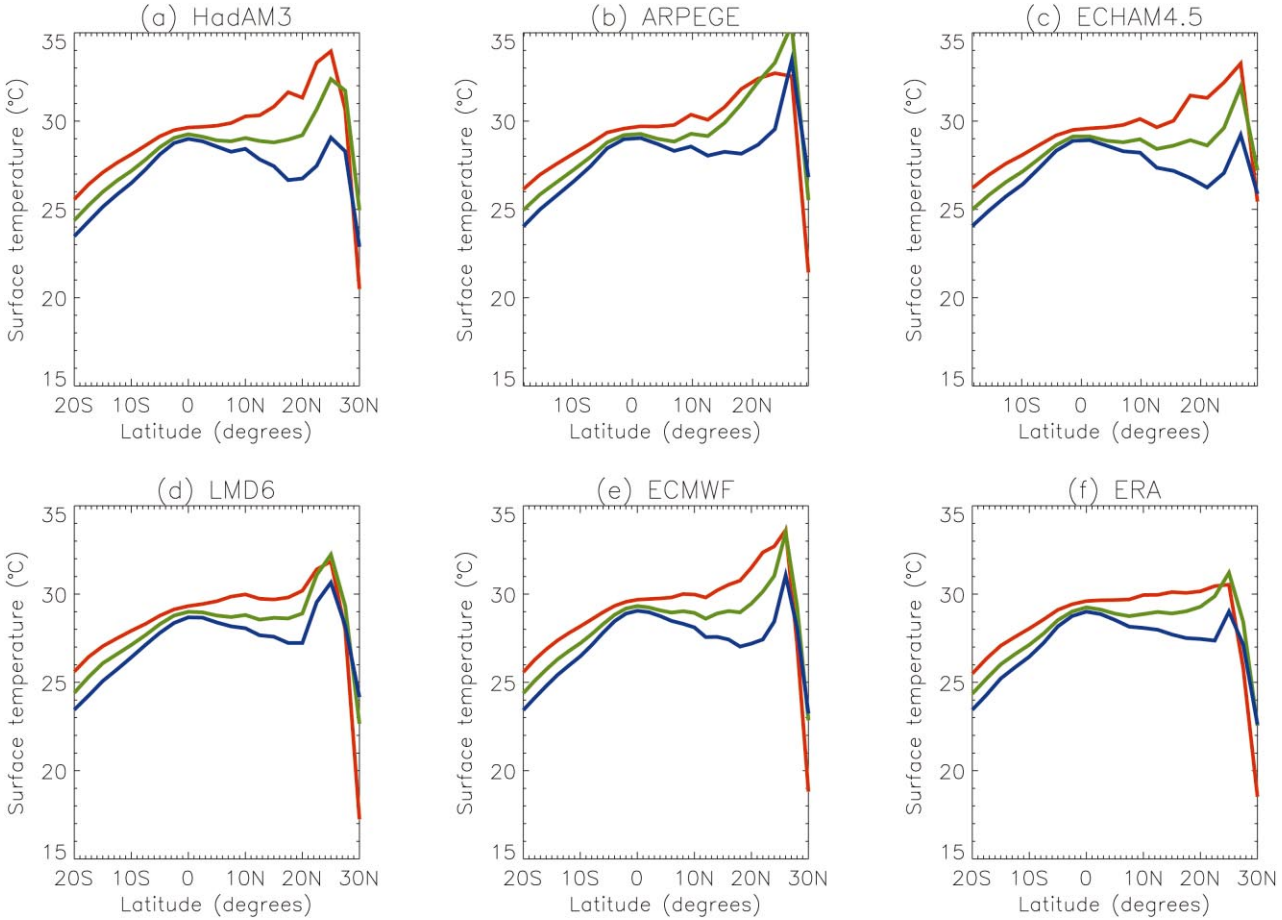

Figure 5. Caption on next page.

early, particularly over India and the Bay of Bengal. The precipitation over these regions is underestimated throughout the season, although the circulation is slightly overestimated at low levels. This may indicate convection which is not deep enough.

5. DEVELOPMENT OF THE MONSOON

The Asian summer monsoon develops in response to large-scale temperature gradients which grow during boreal spring as a result of solar heating of the Asian continent and warming of the northern Indian Ocean. Figure 5(a–f) shows climatological monthly mean surface temperatures in May, June and July, zonally averaged between 60°E and 90°E, for the five SHIVA models and ERA. The SSTs are the

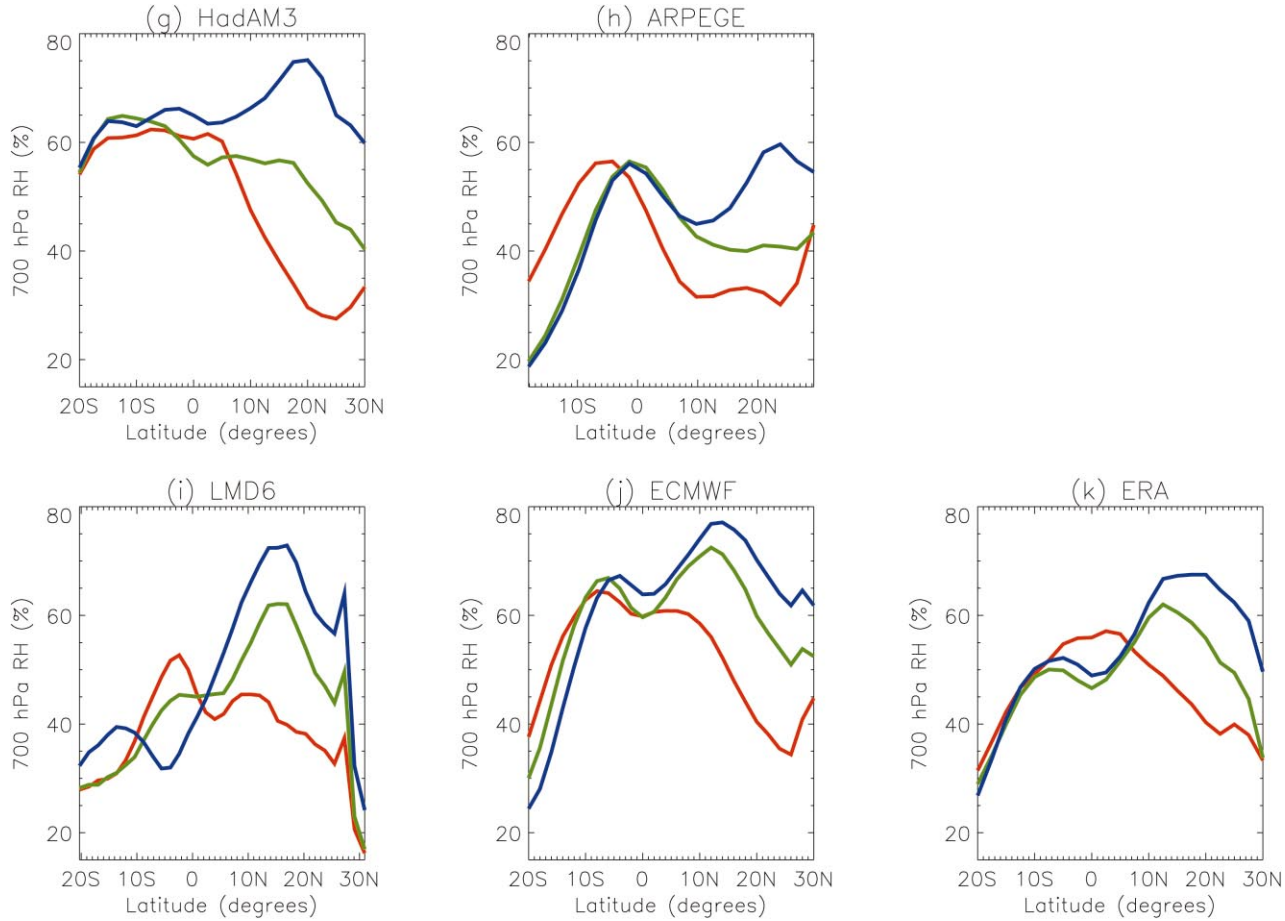

Figure 5. Zonal mean (60–90°E) surface temperature (a–f) and 700 hPa relative humidity (g–k) in May (red), June (green) and July (blue) from the five SHIVA models and ERA.

imposed values. Note that the surface temperatures for HadAM3, ECHAM4.5, LMD6, ECMWF and ERA are skin temperatures whilst that for ARPEGE is the temperature in the first soil layer (with the nature of the soil (e.g. vegetation, snow cover) taken into account). In addition, computation of skin temperature varies between different land surface schemes. Care must be taken in comparing these values quantitatively. However, the evolution of the land–sea temperature contrast as the monsoon develops can be compared between the models.

Both the SST and the land surface temperature are generally greatest in May, but the north-south temperature gradient is also greatest at this time in the models and in ERA. Once the monsoon is established (July), the land surface cools as the soil moisture increases, and the

northern Indian Ocean cools as a result of increased wind-driven mixing and surface evaporation, and reduced insolation (Rao *et al.*, 1989). Meanwhile, the equatorial Indian Ocean SSTs show little change during this three month period. The results from ERA show that the land surface temperatures in the central Indian peninsula are cooler than the equatorial Indian Ocean SSTs in July, although they remain warmer than the SSTs south of the equator. Similar trends are seen in all of the SHIVA models. ARPEGE shows rather less cooling between May and June than the other models, associated with its late monsoon onset as illustrated in Figure 4. However, this model, along with LMD6, shows similar cooling to ERA overall between May and July. This contrasts with HadAM3, ECHAM4.5 and ECMWF, in which there is more precipitation over this region throughout the season (see Figure 3), and in which the cooling over India is much larger.

The development of the monsoon is also associated with a deepening of the moist layer as increasing convective activity transports heat and moisture vertically. Figure 5(g–k) shows the climatological monthly mean relative humidity at 700 hPa in May, June and July, zonally-averaged between 60°E and 90°E, from four of the SHIVA models (relative humidities were not available from ECHAM4.5) and from ERA. The deepening of the moist layer over India between May and July is apparent in the ERA results. This is accompanied by a reduction in relative humidity at this level in the equatorial region as the tropical convergence zone moves northwards. A similar trend of moistening over the Indian peninsula is seen in the models, although the corresponding drying in the equatorial region is not readily apparent. Quantitatively, the results from LMD6 compare fairly well with ERA. In contrast, HadAM3 is too dry over India in May and June, but moistens excessively in July, whilst in ECMWF the relative humidity over India is similar to ERA in May but moister than ERA in June and July. ARPEGE remains too dry compared with ERA in all three months. These differences reflect, to some extent, the errors in monsoon precipitation shown in Figures 3 and 4. The relative humidity to the south of the equator in HadAM3 far exceeds that in ERA and the other SHIVA models. This is related to the error in the location of the convective region over the Indian Ocean, which is too far west in this model compared with observations (see Figure 3).

6. ONSET CHARACTERISTICS

Although the onset of the summer monsoon implies the arrival of the ITCZ over the region, there is some difficulty in defining the actual onset date, particularly since the monsoon exhibits substantial variations in intensity during its advance. In India, the primary indicator of onset has, for many years, been a sharp and sustained increase in rainfall at a group of adjacent stations. However, the occurrence of considerable pre-monsoon thunderstorm activity makes it difficult to identify the monsoon onset in this way, and maps of onset dates are usually drawn with an understanding of the direction that the monsoon typically advances (Asnani, 1993). An objective method for calculating the date of onset across the Asian monsoon region has been proposed by P. Tschuck and M. Cui (personal communication). With this method, onset at a particular location is defined as the first day on which the daily mean rainfall exceeds a local threshold (the long-term July average for that location), provided that the average rainfall over the next five days also exceeds that threshold. In addition, the 850 hPa wind direction is required to be within 45° of the long-term July average direction and the speed exceeding 1 m/s. The mean onset dates from this analysis for each of the model runs and ERA are shown in Figure 6(a–f). It should be noted that this method does not distinguish between monsoon regions and other regions, and a date can almost always be found relative to the long-term July average, regardless of how large that average may be. Thus, in an attempt to omit non-monsoon regions from this analysis, gridboxes where the long-term July average of observed (CMAP/O) rainfall is below 2.5 mm/day have been masked out in Figure 6.

In ERA, the onset date over the southern tip of India is 20 May, and the monsoon can be seen to take about 40 days to progress northwards to Rajasthan. The onset is earliest (before 10 May) over South China, and later (19 June) over the Philippines. Comparison

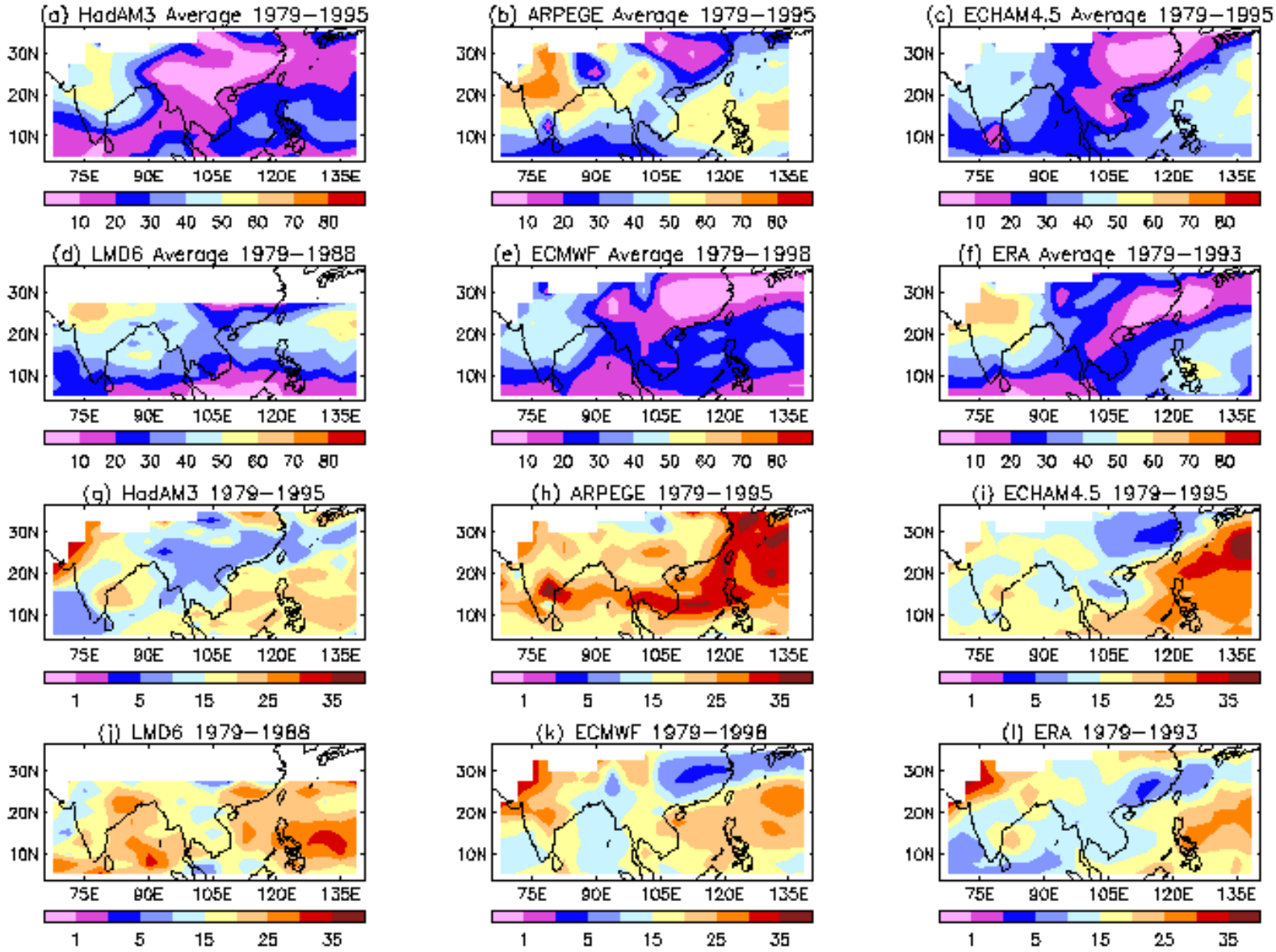

Figure 6. Average (a–f) and standard deviation (g–l) of monsoon onset date (days from 1 May) in the five SHIVA models and ERA. The data have been interpolated onto the grid of the UKMO model.

with other climatologies of onset dates, such as those collected in Asnani (1993), suggests that the onset dates over the Indian and southeast Asian regions, calculated using this method, are in reasonable agreement with accepted normal onset dates (based on precipitation), but that those calculated over South China may be rather early. In this region, pre-monsoon rains occur from mid-April to the end of May, and the summer monsoon itself begins towards mid-June, moving northwards to reach 30°N by the beginning of July. It is possible that the onset date calculated using the method of Tschuck and Cui has captured the onset of pre-monsoon rains in this region. Over the Philippines, the summer monsoon typically first appears in the south during early May, progressing to the north of the region during June. This is consistent with the calculated onset dates shown in Figure 6(f).

The basic pattern of onset dates over India is represented reasonably well by the models. However, the tendency for early onset in HadAM3 and later onset in ARPEGE can be seen throughout the region. The onset is also rather early over the Indian region in ECHAM4.5 and LMD6, although both of these models show reasonable onset dates compared with ERA over the Philippines. In the ECMWF model, the onset dates over southern India and East Asia are in good agreement with ERA, although those over central and northern India and the Philippines are rather early. The rate of northward progression over India in LMD6 is similar to ERA; in ARPEGE it is slightly slower, whilst in HadAM3, ECMWF and ECHAM4.5 it is rather faster, with the monsoon taking only about 30 days to progress from Kerala to Rajasthan. In both ARPEGE and LMD6 the monsoon onset over East Asia is rather late compared with ERA. These two models do not show the large difference in onset date between India and East Asia that is seen in ERA. Instead, the spatial pattern of onset dates is much more zonal. All of the models are fairly consistent with ERA in their analysis of relatively early onset dates over south China. Without further analysis, it is difficult to determine whether this indicates agreement between the models and analysis in terms of the occurrence of pre-monsoon rains over this region. However, the consistency between the models and ERA in determining the first date of occurrence of persistent rainfall and winds which are similar to the July average is encouraging.

Calculation of the standard deviation of the onset dates from ERA (Figure 6(l)) shows values along the southwest coast of India that are in agreement with those suggested by Soman and Kumar (1993). Smaller interannual variability of the monsoon onset date is seen over the Indian peninsula and over East Asia, compared with northern India (in the region of the monsoon trough) and the Philippines. A similar pattern is seen in HadAM3, ECHAM4.5 and ECMWF (Figure 6(g, i and k)), although in the ECMWF model the difference between these regions is smaller than in ERA. In HadAM3 the standard deviations are smaller in magnitude than ERA over East Asia and to the east of the Philippines, and larger than ERA over the South China Sea, whilst those in ECHAM4.5 are similar to or slightly smaller than ERA over the land areas but rather larger than ERA over Indonesia, the Philippines and the western Pacific. The standard deviations of onset date in LMD6 (Figure 6(j)) and, more particularly, in ARPEGE (Figure 6(h)), are much larger than those in ERA, and the values in the Indian region are only slightly less than those further east.

7. SUMMARY

The climatology of the monsoon has been compared between five different GCMs which were used during SHIVA. Long (at least 10 years) model runs forced by observed SSTs and sea ice distributions have been used, and the long-term monthly and seasonal averages have been compared. Although we have highlighted known systematic errors and the impact of recent model developments, no attempt has been made to explain the reasons for differences between the monsoon climatologies from each of the models. This is because the models differ considerably, in horizontal and vertical resolution, numerical schemes and physical parametrizations, so that it is impossible to isolate the cause of differences in their monsoon simulations. The purpose of this comparison is to document and compare the representation of the

mean monsoon in models which are being used to investigate the characteristics of the monsoon, its variability and its response to different boundary forcings.

All of the models produce a reasonable representation of the monsoon circulation, although there are regional variations in the magnitude and pattern of the flow at both 850 hPa and 200 hPa. Two of the models (HadAM3 and LMD6) overestimate the strength of the monsoon circulation considerably. The others tend to underestimate the magnitude of the upper level easterly winds. Considerable differences between the models are seen in the amount and distribution of precipitation, with HadAM3, ECHAM4.5 and ECMWF rather overactive in the Indian region whilst ARPEGE tends to underestimate in this region, and LMD6 being far more active in the western Pacific. The models all reproduce the basic monsoon seasonal variation, although the timing of the onset and retreat, and the maxima in the winds and precipitation during the established phase, differ between them. There are corresponding differences in the evolution of the atmospheric structure between the pre-monsoon season and its established phase.

This study illustrates the variations in the quality of different aspects of the Asian summer monsoon simulation between five different models. The complexity of the Asian monsoon system and its variability, combined with the regional nature of the precipitation distribution and the importance of this to the economies of the countries under its influence, make the accurate simulation of the monsoon an essential but challenging requirement in global climate modelling. It is hoped that this study will set in context the investigations of the monsoon system and its impacts carried out using these models, both during SHIVA and in the future.

Acknowledgements

This work was carried out under the Studies of the Hydrology, Impact and Variability of the Asian summer monsoon (SHIVA) project, funded by European Union contract no. ENV4-CT95-0122. We are grateful to the Coordinator, Dr Julia Slingo, for her help and advice during this project.

REFERENCES

Annamalai, H., Slingo, J. M., Sperber, K. R. and Hodges, K., 1999. The mean evolution and variability of the Asian summer monsoon: Comparison of ECMWF and NCEP/NCAR reanalyses. *Mon. Weather Rev.*, **127**, 1157–1186.

Asnani, G. C., 1993. *Tropical Meteorology*. G.C. Asnani, Pune, India. xvi + 603 pp.

Beljaars, A. C. M. and Viterbo, P., 1998. The role of the boundary layer in a numerical weather prediction model. In *Clear and Cloudy boundary layers*, Holtslag, A. A. M. and Duynkerke, P. G., Eds. North-Holland Publishing Company, Amsterdam, 287–304.

Bougeault, P., 1985. A simple parameterization of the large-scale effects of cumulus convection. *Mon. Weather Rev.*, **113**, 2108–2121.

Cox, P. M., Betts, R. A., Bunton, C., Essery, R. L. H., Rowntree, P. R. and Smith, J., 1999. The impact of new land surface physics on the GCM simulation of climate and climate sensitivity. *Clim. Dyn.*, **15**, 183–203.

Ducoudre, N., Laval, K. and Perrier, A., 1993. SECHIBA, a new set of parametrizations of the hydrological exchanges at the land/atmosphere interface within the LMD atmospheric general circulation model. *J. Climate*, **6**, 248–273.

Edwards, J. and Slingo, A., 1996. Studies with a flexible new radiation code. I: Choosing a configuration for a large-scale model. *Q. J. R. Meteorol. Soc.*, **122**, 689–720.

Ferranti, L., Slingo, J. M., Palmer, T. N. and Hoskins, B. J., 1999. The effect of land surface feedbacks on the monsoon circulation. *Q. J. R. Meteorol. Soc.*, **125**, 1527–1550.

Fouquart, Y. and Bonnel, B., 1980. Computation of solar heating of the earth's atmosphere: A new parametrization. *Beitr. Phys. Atmos.*, **53**(1), 35–62.
Gadgil, S. and Sajani, S., 1998. Monsoon precipitation in the AMIP runs. *Clim. Dyn.*, **14**, 659–689.
Gates, L. W., 1992. AMIP: the Atmospheric Model Intercomparison Project. *Bull. Am. Meteorol. Soc.*, **73**, 1962–1970.
Gibson, J. K., Kallberg, P., Uppala, S., Hernandez, A., Nomura, A. and Serrano, E., 1997. ERA description. ECMWF Re-Analysis Project Series, 1. Available from the European Centre for Medium-range Weather Forecasting (ECMWF), Shinfield Park, Reading, U.K.
Gregory, D. and Rowntree, P. R., 1990. A mass flux convection scheme with representation of cloud ensemble characteristics and stability dependent closure. *Mon. Weather Rev.*, **118**, 1483–1506.
Gregory, D., Kershaw, R. and Inness, P. M., 1997. Parametrization of momentum transport by convection. II: Tests in single-column and general circulation models. *Q. J. R. Meteorol. Soc.*, **123**, 1153–1183.
Martin, G. M. and Soman, M. K., 1999. Effects of changing physical parametrisations on the simulation of the Asian summer monsoon in the U.K. Meteorological Office Unified Model. Hadley Centre Technical Note No. 17, Hadley Centre, The Met. Office, London Road, Bracknell, U.K.
Morcrette, J. J., Smith, L. and Fouquart, Y., 1986. Pressure and temperature dependence of the absorption in longwave radiation parameterizations. *Beitr. Phys. Atmos.*, **59**, 455–469.
Morcrette, J., 1990. Parametrization of radiation transfer in the ECMWF model. Proceedings of ECMWF Seminar: ''Ten years of medium-range weather forecasting'', 4–8 September 1989. Volume II, pp. 93–13. Available from ECMWF, Shinfield Park, Reading, UK. Morcrette, J., Smith, L. and Fouquart, Y., 1986. Pressure and temperature dependence of the absorption in longwave radiation parametrizations. *Beitr. Phys. Atmos.*, **59**, 455–468.
Noilhan, J. and Planton, S., 1989. A simple parameterization of land surface processes for meteorological models. *Mon. Weather Rev.*, **117**, 536–549.
Polcher, J. and Laval, K., 1994. A statistical study of the regional impact of deforestation on climate in the LMD GCM. *Clim. Dyn.*, **10**, 205–219.
Pope, V. D., Gallani, M., Rowntree, P. R. and Stratton, R. A., 2000. The impact of new physical parametrizations in the Hadley Centre climate model—HadAM3. *Clim. Dyn.*, **16**, 123–146.
Rao, R. R., Molinari, R. L. and Festa, J. R., 1989. Evolution of the climatological near-surface thermal structure of the tropical Indian Ocean. Description of the mean monthly mixed layer depth, and sea surface temperature, surface current and surface meteorological fields. *J. Geophys. Res.*, **94**, 10801–10815.
Rayner, N. A., Horton, E. B., Parker, D. E., Folland, C. K. and Hackett, R. B., 1996. Version 2.2 of the Global Sea-Ice and Sea Surface Temperature data set, 1903–1994. Climate Research Technical Note No. 74, Hadley Centre, Meteorological Office, London Road, Bracknell, RG12 2SY, U.K.
Ricard, J.-L. and Royer, J.-F., 1993. A statistical cloud scheme for use in an AGCM. *Annales Geophysicae*, **11**, 1095–1115.
Roeckner, E., Arpe, K., Bengtsson, L., Brinkop, S., Dumenil, L., Esch, M., Kirk, E., Lunkeit, F., Ponater, M., Rockel, B., Sansen, R., Schlese, U., Schubert, S. and Windelband, M., 1992. Simulation of the present-day climate with the ECHAM model: impact of model physics and resolution Report No. 93. Max-Planck-Institute for Meteorology, Hamburg, 171 pp.
Roeckner, E., Arpe, K., Bengtsson, L., Christoph, M., Claussen, M., Dumenil, L., Esch, M., Giorgetta, M., Schlese, U. and Schulzweida, U., 1996. *The atmospheric general circulation model ECHAM-4: Model description and simulation of present-day climate. Report No. 218.* Max-Planck-Institute for Meteorology, Hamburg, 90 pp.
Slingo, J. M. et al. 1999. *SHIVA Final Report: March 1996–February 1999.* Published by the European Commission and available free of charge from the Office for Official Publications of the European Communities, L-2985 Luxembourg, ISBN 92-828-7758-2.
Smith, R. N. B., 1990. A scheme for predicting layer clouds and their water content in a General Circulation Model. *Q. J. R. Meteorol. Soc.*, **116**, 435–460.
Soman, M. K. and Kumar, K. K., 1993. Space-time evolution of meteorological features associated with the onset of Indian summer monsoon. *Mon. Weather Rev.*, **121**, 1177–1194.
Stephenson, D. B., Chauvin, F. and Royer, J.-F., 1998. Simulation of the Asian summer monsoon and its dependence on model horizontal resolution. *J. Met. Soc. Japan*, **76**, 237–265.
Tiedtke, M., 1993. Representation of clouds in large-scale models. *Mon. Weather Rev.*, **121**, 3040–3061.

Viterbo, P. and Beljaars, A. C. M., 1995. An improved land surface parameterization scheme in the ECMWF model and its validation. *J. Climate*, **8**, 2716–2748.

Xie, P. and Arkin, P. A., 1997. Global precipitation: a 17-year monthly analysis based on gauge observations, satellite estimates and numerical model outputs. *Bull. Am. Meteorol. Soc.*, **78**, 2539–2558.